Vibration measurements of a laboratory-scale ladle

HAMK
HÄMEEN AMMATTIKORKEAKOULU
HÄME UNIVERSITY OF APPLIED SCIENCES

Bachelor's thesis

Mechanical engineering

Autumn 2022

Matias Hauru

HAMK
HÄMEEN AMMATTIKORKEAKOULU
HÄME UNIVERSITY OF APPLIED SCIENCES

ABSTRACT

Konetekniikka
Riihimäki

Author Matias Hauru **Year** 2022

Title Laboratoriokokoisen senkan värähtelymittaukset

Supervisor(s) Timo Kärppä (HAMK), Ville-Valtteri Visuri (Oulun Yliopisto), Mika Pylvänäinen (Oulun Yliopisto)

Tämän opinnäytetyön tavoitteena oli selvittää, vaikuttaako kuonakerroksen paksuus senkan värähtelyyn kaasusekoituksen aikana. Tutkimus tehtiin laboratorioympäristössä 1:5-mittakaavan vesimallilla, joka kuvaa oikeaa 150 tonnin senkkaa. Vesimallissa senkkahuuhtelua simuloitiin ilmalla, vedellä ja rypsiöljyllä, jotka kuvaavat argonia, sulaa terästä ja kuonaa. Senkan värähtelyn mittaamiseksi suoritettiin mittauskampanja käyttäen kahdeksaa kiihtyvyysanturia, jotka oli kiinnitetty eri puolille senkan seinämää. Mittauskampanjan tuloksista koostettiin aineisto, jonka avulla voitiin tutkia öljykerroksen paksuuden vaikutusta senkan värähtelykäyttäytymiseen.

Tämä opinnäytetyö tehtiin Oulun yliopiston Älykkäät koneet ja järjestelmät ja Prosessimetallurgian tutkimusyksiköille, jatkona edelliselle tutkimukselle, jossa keskityttiin kiihtyvyysantureiden lukumäärän ja sijaintien optimointiin teollisuussovelluksissa ja senkanvalvontajärjestelmissä.

Työn tulosten perusteella selvisi, että öljykerroksen paksuus vaikuttaa värähtelyn voimakkuuteen tavalla, joka voidaan tunnistaa kiihtyvyysantureilla. Tuloksista ilmeni myös, että mitattu värähtelyn voimakkuus riippuu kiihtyvyysantureiden sijainnista. Lähellä suutinta ja kaasuvirtausta olevat kiihtyvyysanturit ovat herkempiä prosessiparametrien muutoksille kuin vastakkaisella puolella olevat kiihtyvyysanturit.

Avainsanat Teräksenvalmistus, senkka, värähtely, kuona

Sivut 23 sivua

HAMK
HÄMEEN AMMATTIKORKEAKOULU
HÄME UNIVERSITY OF APPLIED SCIENCES

ABSTRACT

Mechanical engineering
Riihimäki

Author Matias Hauru **Year** 2022

Subject Vibration measurements of a laboratory-scale ladle

Supervisor(s) Timo Kärppä (HAMK), Ville-Valtteri Visuri (University of Oulu), Mika Pylvänäinen(University of Oulu)

The aim of this thesis was to study whether the thickness of the slag layer affects the vibration of the ladle during gas stirring. The study was conducted in a laboratory environment using a 1:5 scale water model of an actual 150-tonne ladle. In the water model, the gas stirring process was simulated with air, water and rapeseed oil representing argon, molten steel, and slag. A measurement campaign was carried out to measure the ladle vibrations using eight accelerometers attached to different parts of the ladle wall. The results of the measurement campaign were used to compile a dataset to investigate the effect of the oil layer thickness on the vibration behavior of the ladle.

This thesis was carried out for the Intelligent Machines and Systems and Process Metallurgy research units of the University of Oulu as a continuation of a previous study focusing on optimizing the number and location of accelerometers in industrial applications and ladle monitoring systems.

The results of the study showed that the thickness of the oil layer affects the vibration intensity in a way that can be detected by accelerometers. The results also showed that the measured vibration intensity depends on the accelerometers' location. Accelerometers close to the nozzle and gas flow are more sensitive to changes in process parameters than accelerometers on the opposite side.

Keywords Steelmaking, ladle, vibrations, slag

Pages 23 pages

CONTENTS

USED SYMBOLS AND ABBREVIATIONS

C°	Celsius
l	Liter
rpm	Rounds per minute
Pa·s	Pascal second
m/s^2	Meters per second squared
Hz	Hertz
mV/g	Millivolts or per g
RMS	Root mean square

DEFINITIONS

Accelerometer	Device that measures acceleration forces. These forces might be static, such as the steady force of gravity, or dynamic, like those created by the accelerometer moving or vibrating.
Ladle	A bucket-like tank lined with refractory bricks and used in steelmaking to transport molten steel from one process stage to another.
Ladle treatment	Process stage, which aims to match the composition and temperature of the steel and remove impurities.
Open eye	Gas injected from the bottom of the ladle into the steel melt pushes the slag aside, creating a clear area to the top phase. A clear area created in the top phase is called an “open eye”.
Slag	A solution consisting mainly of molten oxides. Fluxes, such as calcium oxide (CaO), can be added to the melt to enhance the accumulation of contaminants in the slag.

1 INTRODUCTION

Ladle treatment is part of the secondary metallurgy of steelmaking. This process aims to homogenize and fine-tune the composition and temperature of the steel melt before continuous casting by injecting gas from the bottom of the ladle through one or several purging plugs. Because of gas leakage or plug blockage, the stirring process is hard to manage due to the inconsistent stirring strength. (Anagbo;Brimacombe;& Castillejos, 1989)

The aim of this work is to run a measurement campaign to gather a dataset of the ladle vibration and record the formation of an open eye during gas stirring. The experiment will be conducted in a laboratory environment with a 1:5 scale water model. In the experiment, the stirring process is simulated with an acrylic ladle, where air, water, and rapeseed oil represent argon, liquid steel, and slag. The ladle vibrations will be measured with eight mono-axial accelerometers. The accelerometers are placed in different positions on the ladle wall to measure ladle vibrations simultaneously. The dataset and video recordings obtained can be studied to determine whether the thickness of the surface phase can be determined by ladle vibration and how much the thickness of the surface phase affects the formation of an open eye. This work does not analyse the collected vibration data, nor the recorded video clips.

The following research question was set for this work: is the vibration behaviour of the water model affected by the thickness of the oil layer? The obtained results can be used as a reference or a base for future studies considering ladle vibrations, relating to the design of ladle monitoring systems based on accelerometers and better identifying the operating conditions during ladle treatments.

This thesis is made for the Intelligent Machines and Systems and the Process Metallurgy Research Unit at the University of Oulu as a continuation of an earlier study (Alia, et al. 2019), which focused on optimizing the number and placement of accelerometers in industrial applications and ladle monitoring systems.

2 SECONDARY METALLURGY

Secondary metallurgy deals with the development of materials used by industry, including the production of alloys, thermomechanical treatments (rolling, quenching, tempering), and shaping into semi-finished products (plates, profiles). In general, secondary metallurgy refers to ladle treatments. Ladle treatments are those metallurgical operations between a converter and continuous casting as the steel melt is transported in a ladle from one process step to another (Figure 1). The process steps depend on the type of steel produced. For example, the manufacturing process for stainless steel is different from that for steel, so the process steps are different. However, the aim is the same, regardless of the steel to be produced. The main objective is to adjust the composition, i.e. add alloys and remove impurities, match the temperature, because the added alloys affect the melting temperature of the steel when

casting, and homogenize the molten steel to obtain uniform compositions and temperature. (Stolte, 2002, pp. 13-17)

Figure 1 Steps in ladle treatment (O'Malley, 2017)

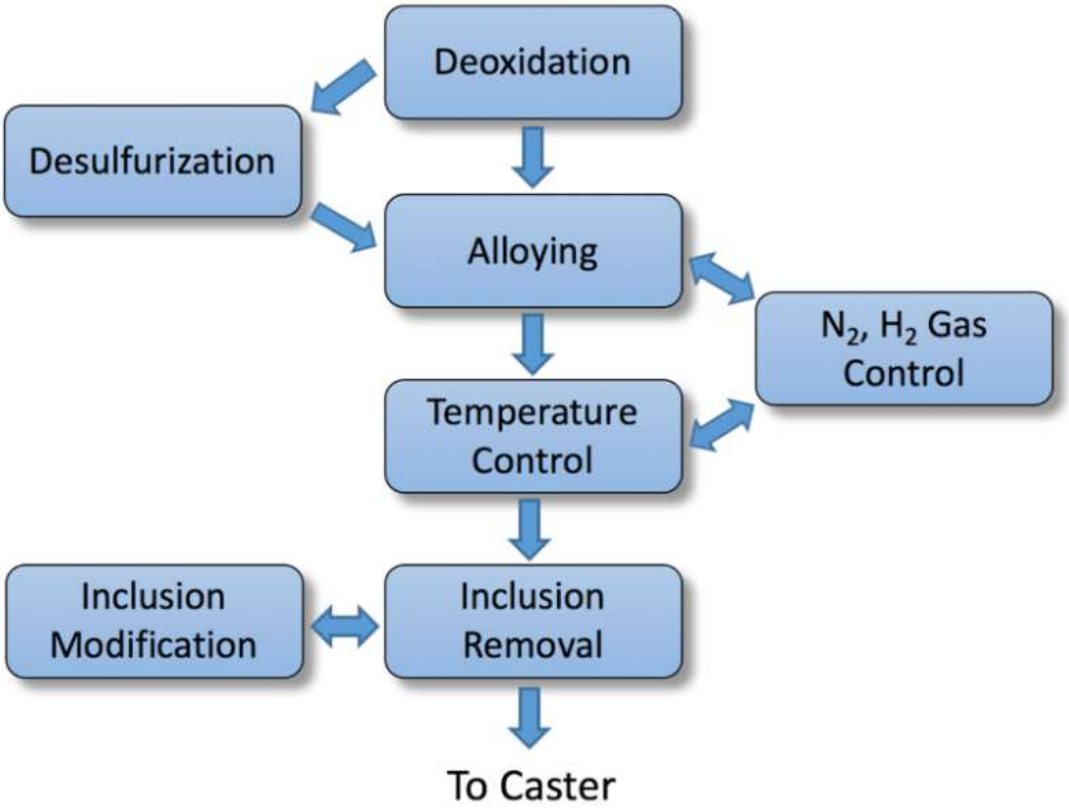

2.1 **Composition control**

The basic steps in the refining steel include desulphurization, decarburization, and modification of inclusions, which involve the removal of harmful gases and non-metallic inclusions, as well as raising the temperature and adjusting the composition of the molten steel. Scrap-based steelmaking, on the other hand, requires melting in an electric arc furnace.

2.1.1 Decarburization

In the basic oxygen furnace (BOF) process, the carbon level is reduced to the desired amount by burning off the excess carbon. Decarburization, i.e., carbon removal is carried out in a basic oxygen furnace. In the BOF, oxygen is added to the melt. The injected oxygen begins to react with the molten steel. The reaction produces carbon monoxide gas, which is removed from the process. (Metallinjalostajat ry, 2014)

There are three types of decarburization processes (Figure 2a, 2b, 2c): the LD method, the OBM method, and the combined blowing method. The LD method is the most traditional of the oxygen-blowing processes. In this process, oxygen is blown through a lancet that descends from above the converter. The oxygen jet is spread over the steel

alloy through holes at the end of the lancet. In the OBM blowing method or bottom blowing, oxygen is blown through nozzles located at the bottom of the converter. The nozzles are ring nozzles formed by two nested tubes. The OBM and LD methods are very similar. Modern converters are combined-blowing converters. LD converters are equipped with bottom nozzles that blow inert gas and OBM converters are equipped with top nozzles (Metallinjalostajat ry, 2014).

Figure 2 Oxygen furnaces a) OBM method b) LD method c) compound method d) AOD method (Metallinjalostajat ry, 2014)

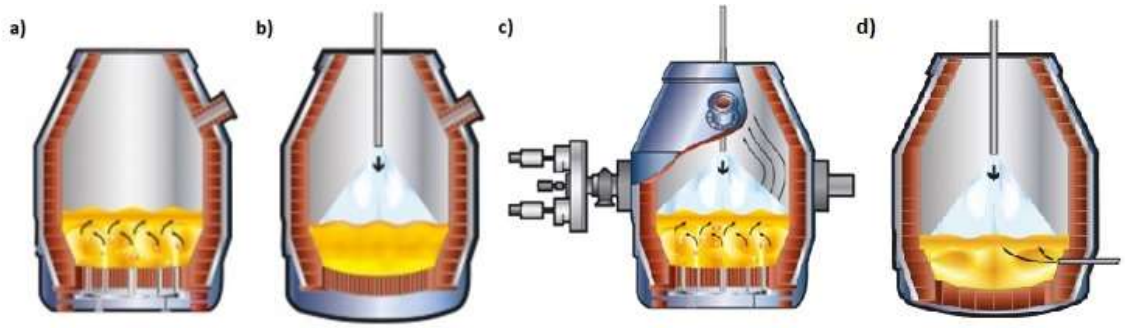

In stainless steelmaking, the most common method for decarburization is an argon-oxygen-decarburization (AOD) converter (Figure 2d). AOD-converter is a vessel lined with refractory bricks into which the process gases are fed through the walls via nozzles installed at the bottom of the converter. In the AOD process, decarburization is carried out with a mixture of oxygen and inert gas. The inert gas is used to reduce the partial pressure of the carbon monoxide produced during the decarburization process, thus promoting the decarburization reaction. (Metallinjalostajat ry, 2014)

2.1.2 Deoxidation

During decarburization, part of the oxygen injected dissolves into the steel bath. If oxygen-rich steel is being cast, gas bubbles are formed, which, when solidified, create a porous surface, and some of the oxygen or carbon monoxides in the bubbles are trapped in the solidified steel. For this reason, oxygen must be removed from the steel before solidification. Deoxidation means that a substance with high oxygen affinity is added to molten steel. The most common high oxygen affinities are aluminum, silicon, and manganese. These substances can be fed as a wire into the melt, for example as shown in Figure 3. In wire feeding, a thin-walled steel tube, i.e. wire, filled with alloying elements is fed into a steel ladle. As the wire enters the melt, its wall begins to melt and the alloying powders are dispersed into the melt, causing the desired reactions. The substances are usually added at the stage when the melt is drained from the primary furnace to a ladle (Szekely, Carlsson, & Helle, 1989, pp. 118-124).

Figure 3 Wire feeding (Metallinjalostajat ry, 2014)

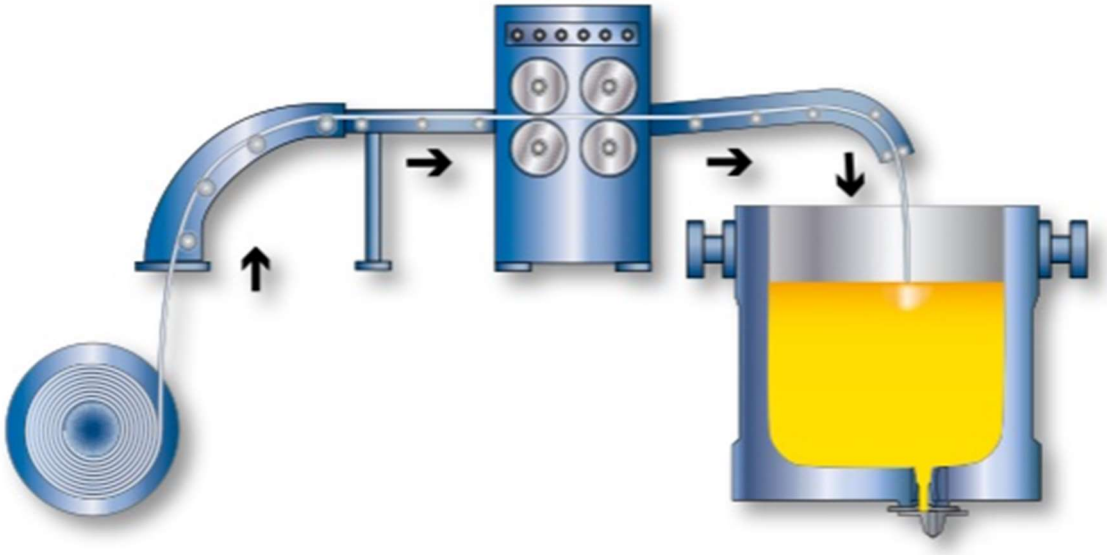

2.1.3 Alloying

Alloying is usually carried out in a converter after blowing or pouring. Preliminary alloying is then performed, which is generally not very accurate in terms of intake, i.e. alloying slightly below the target composition. Some elements are challenging to remove in large quantities. The final composition of the mixture is made after pouring during the ladle treatments. The final or more accurate alloying is done separately because the alloying materials are more expensive than the materials used in the preliminary alloying, and their use takes more time.

Alloying can be carried out with the CAS-OB method (Composition Adjustment by Sealed Argon Bubbling – Oxygen Blowing). CAS-OB is mainly used for chemical heating but can be also used for more accurate alloying.

Figure 4 Parts of the CAS-OB station. 1. Supersonic O2 lance, 2. Dedusting duct, 3. Al-feeding pipe, 4. Surface slag, 5. Ladle, 6. Porous plug for Argon bottom stirring, 7. Steel, 8. Bell, 9. Lance lifting system and 10. Bell lifting system. (Järvinen, et al., 20

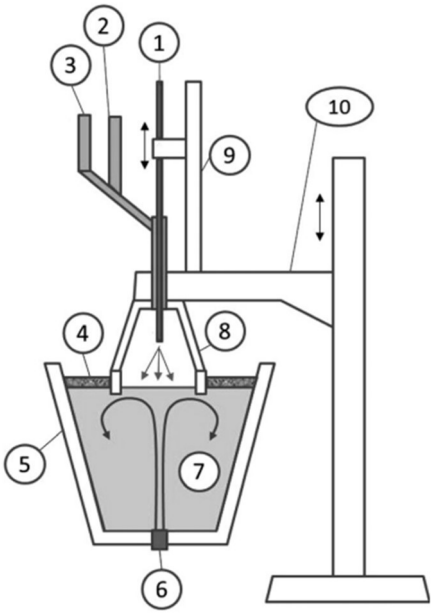

During CAS-OB treatment (Figure 4), argon is injected from the bottom of the ladle into the steel melt, forming an "open eye" on the top phase. After the ''open eye '' has formed, a lance is placed on top of the clear area, and through it, alloying elements are mixed into steel melt. The lance is also used to blow oxygen to the surface. When aluminium is added simultaneously, aluminium oxide is generated, and a notable amount of thermal energy is used to melt the alloying elements. The resulting Al_2O_3 rises to slag. (Metallinjalostajat ry, 2014)

2.2 **Temperature control**

The steel must not solidify before the casting process. The aim is that when the steel enters the casting process, its temperature is just above the limit at which solidification begins. To get the steel hot enough during casting, either the steel can be heated in the converter to a sufficiently high temperature, or in long-duration ladle treatments, temperature control can be carried out in the steel ladle (Figure 5).

Figure 5 Three different ladle treatment stations (Britannica, 2021)

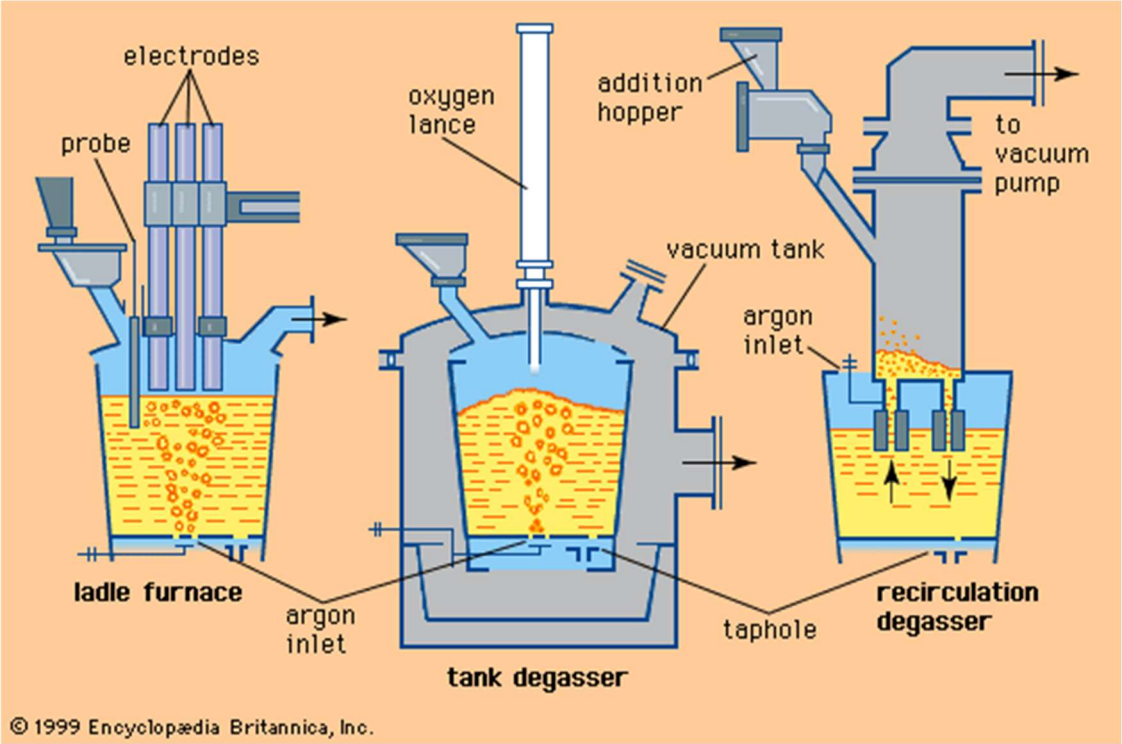

The first starting point for temperature control in a steel ladle is to minimize heat loss by, for example, using covers and select slags that act as insulators. For longer-term ladle treatments, heating is usually required to avoid overheating in the converter. Heating methods may include the CAS-OB method mentioned in Chapter 2.1.2, burners or ladle furnaces that operate in the same way as an electric arc furnace. If the melt needs to be cooled, the most common method is to add scrap iron to the melt. (Stolte, 2002, pp. 99-113)

2.3 **Gas-stirring**

The stirring can be done electromagnetically/inductively to create currents in the steel melt, causing the melt to mix and the composition and temperature to homogenize. (Heikkinen, 2021) A more common stirring method is to inject gas, either from the top with a lance or through bottom nozzles located either in the center of the ladle or eccentrically on the sides. When gas is injected into the melt, gas bubbles are formed, which grow as they rise to the surface. This is due to the pressure at the bottom of the ladle. The pressure decreases the closer you get to the surface, which causes the bubbles to enlarge. During its ascend in the metal bath, temperature of the injected gas rises to match that of the molten steel, which lowers the pressure and causes the bubbles to increase in size. (Ramasetti, 2019)

Figure 6 Three different stirring methods (Heikkinen, 2021)

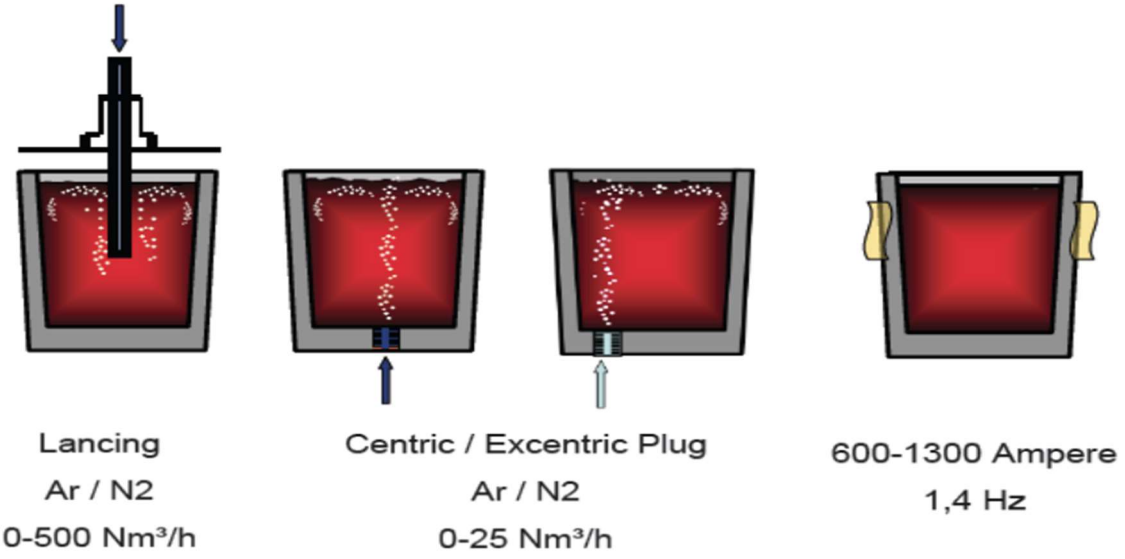

The movement of the gas bubbles through the melt causes the kinetic energy of the gas to be converted into mixing energy. For gas stirring, gases should be selected so that they do not cause deterioration in the quality of the steel. For example, argon is a good option, an inert gas that does not react in this system. Another option is to use nitrogen because it is cheaper. The use of nitrogen in gas stirring causes an increase in the nitrogen level of the steel, but some steels are critical with nitrogen level, so its use as a stirring gas is limited. (Stolte, 2002, pp. 17-22)

3 MATERIALS AND METHODS

3.1 Design of experiment

The main objective of the study is to produce more detailed data related to ladle vibration during gas-stirring. The design of the experiment was created by combining two designs of experiments. In the first one, the oil layer thickness of 0 cm is made by randomizing three air volume flows so that five repetitions are obtained. In the second, oil layer thicknesses of 3, 6, and 9 cm were chosen using a definitive screening test design (Jones & Nachtsheim, 2017) in five repetitions.

Values from previous research (Alia, et al. 2019) were selected for the design of the experiment, as well as values relevant to the research question. Unlike the previous one, in this study, the water surface was kept constant at the height of 54 cm, and the variable was the height of the surface phase, i.e. the thickness of the oil layer. Air currents were previously 5, 10, 15, 20, 25, and 30 Nl/min, and in this study, the flows were limited to 5, 17.5, and 30 Nl/min to reduce the number of tests.

In the final design of the experiment, the total number of tests was 89 (Appendix 1). The test order was created so that there is no need to remove liquid from the water model, but as the test progress, the surface level rises. At the beginning of the new surface height, the specific oscillation frequency was measured by hitting the edge of the water model ten times with a mass hammer.

Tests without oil were added to the test plan to ensure reliable data when data is being analyzed. In these tests, the water level was raised to the same height as the liquid level used in the oil tests. The runs were performed with each airflow, and the specific oscillation frequency was recorded for each height. Water runs can be used to determine whether the vibration of a ladle is mainly affected by the thickness of the oil layer or the height of the liquid surface in general.

Throughout the whole series of tests, the liquid temperature for water and oil was kept at 20°C (±1°C).

Table 1. Example of the first tests of the design of experiment

Test number	Oil-layer thickness (cm)	Volumetric flow rate of air (Nl/min)
HIT 1	0	NO
1	0	30
2	0	17.5
3	0	17.5
4	0	17.5
5	0	30
6	0	5
7	0	5
8	0	17.5
9	0	5
10	0	5
11	0	30
12	0	30
13	0	5
14	0	30
15	0	17.5
16	0.3	19.4
17	1	5.6
18	1.9	25.5
HIT 5	3	NO
19	3	17.5
20	3	30

3.2 **Water model**

To accurately simulate an industrial setting, the water model used in this thesis (Figure 7) is on a 1:5 scale compared to an actual 150-ton ladle. This model was made for research considering the mixing time and size of the open eye during gas injection (Palovaara, 2017). Table 2 and Figure 8 show the specifications of the water model used and Figure 9 shows the orientation of the water tank.

Figure 7 The water model used in the study

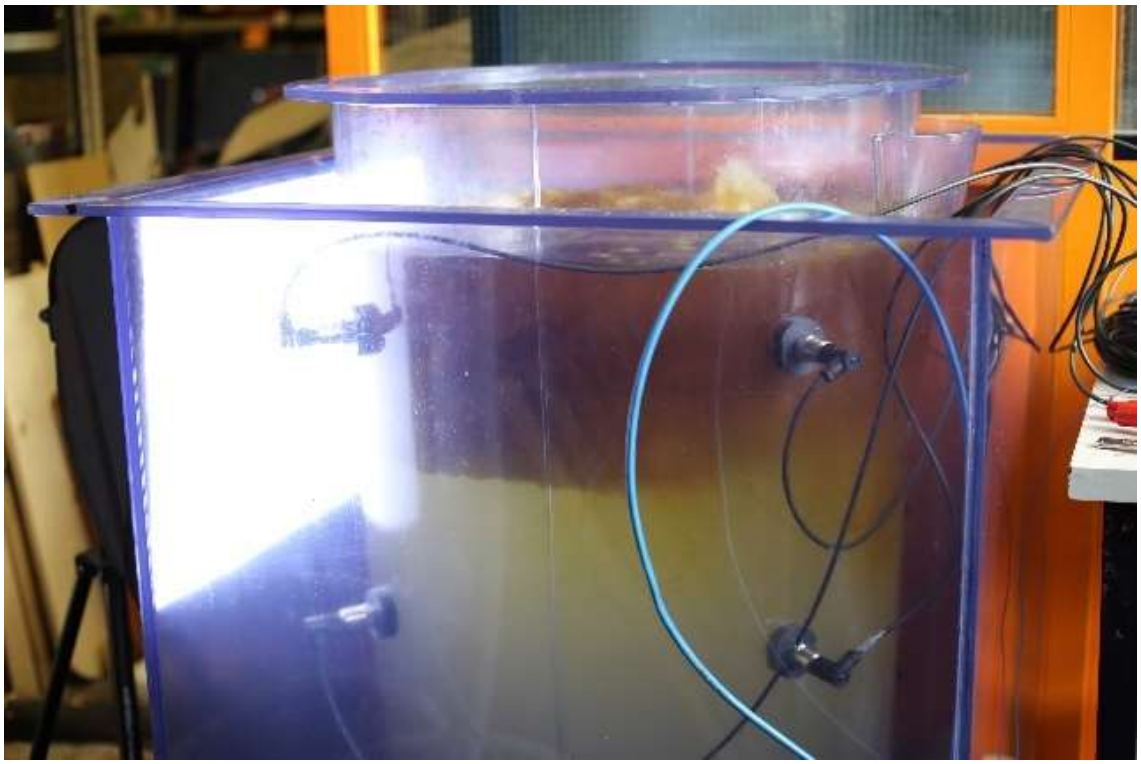

The same water model was used in other studies considering ladle vibrations and open eye, i.e., (Alia, et al. 2019) (Ramasetti, et al. 2018) (Palovaara;Visuri;& Fabritius, 2018).

Table 2. Dimensions of the model (Palovaara, 2017)

Measurement	Variable	Unit
Height of the model	h_m	cm
Height of the bottom step	h_s	cm
Height from the bottom to lip	h_b	cm
Height of the lip	h_l	cm
Diameter of the bottom	$d_{m,\,bottom}$	cm
Diameter of the top	$d_{m,\,top}$	cm
Length of the lip	l_l	cm
The radius of the bottom	R_m	cm
Nozzles distances from the center	$0.55R_m$	cm

Figure 8 Dimensions of the model. X are air injection nozzles, and + is a drain hole (Palovaara, 2017)

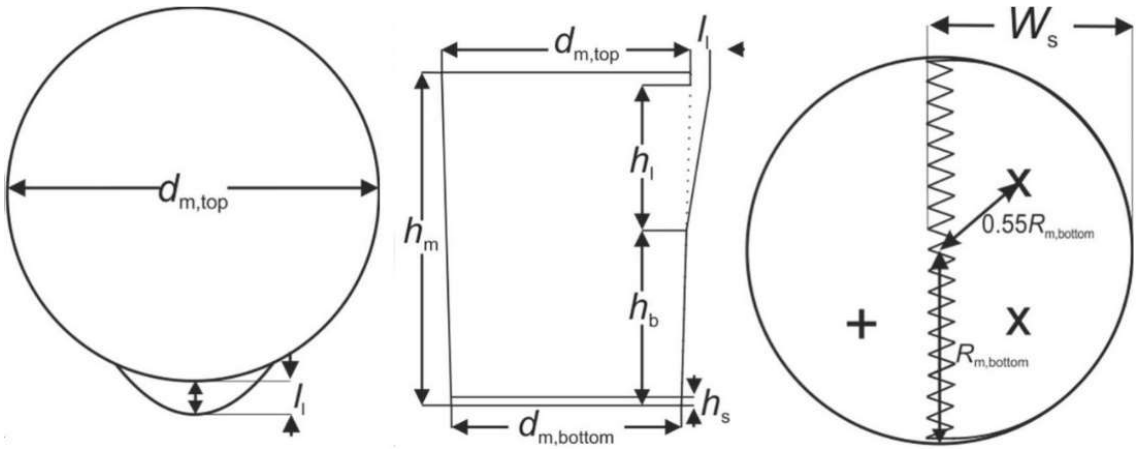

Figure 9 Water model orientations, nozzles' positions and the water height used in the campaign (H = 54cm) a) top view b) perspective view (Alia, et al. 2019)

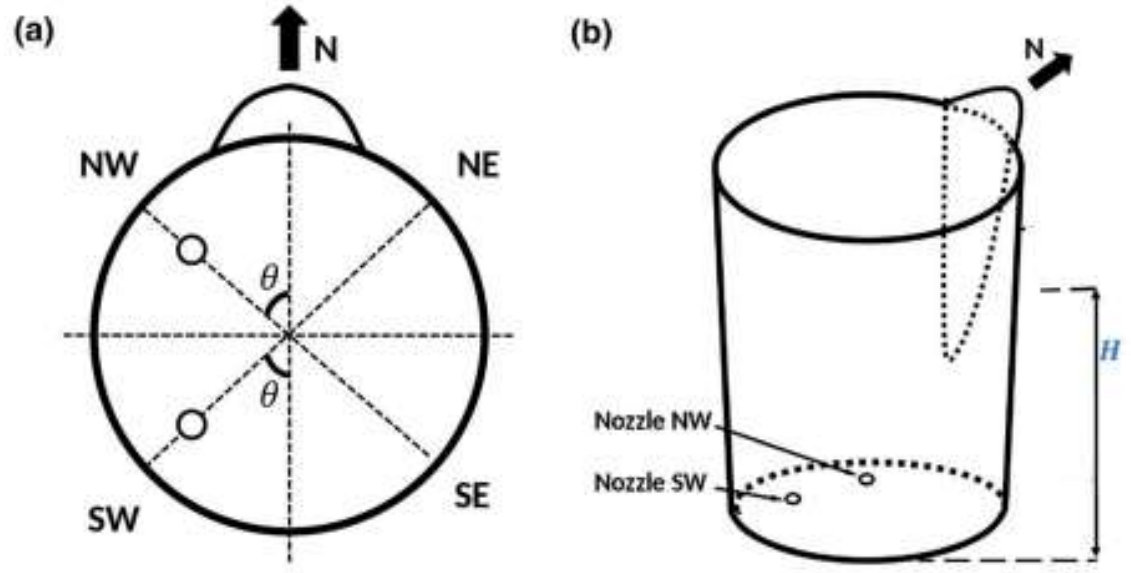

To provide consistency with the previous experiments, the same materials had to be selected for this study. To ensure similar kinematic viscosity, water, rapeseed oil and air were used to represent molten steel, slag, and argon. As a bottom phase, water is a widely used option to portray molten steel because of its suitable kinematic viscosity and valuable properties. Rapeseed oil is a good option for the top phase because of its accessibility, relatively low price, and kinematic viscosity.

3.3 **Oil viscosity**

The viscosity of the rapeseed oil used in the study was measured in the laboratory of The Fiber and Particle Engineering Research Unit at the University of Oulu. The viscosity was measured using a Brookfield DV-II+Pro EXTRA viscometer (Figure 10).

Figure 10 Rapeseed oil viscosity measurement at the University of Oulu

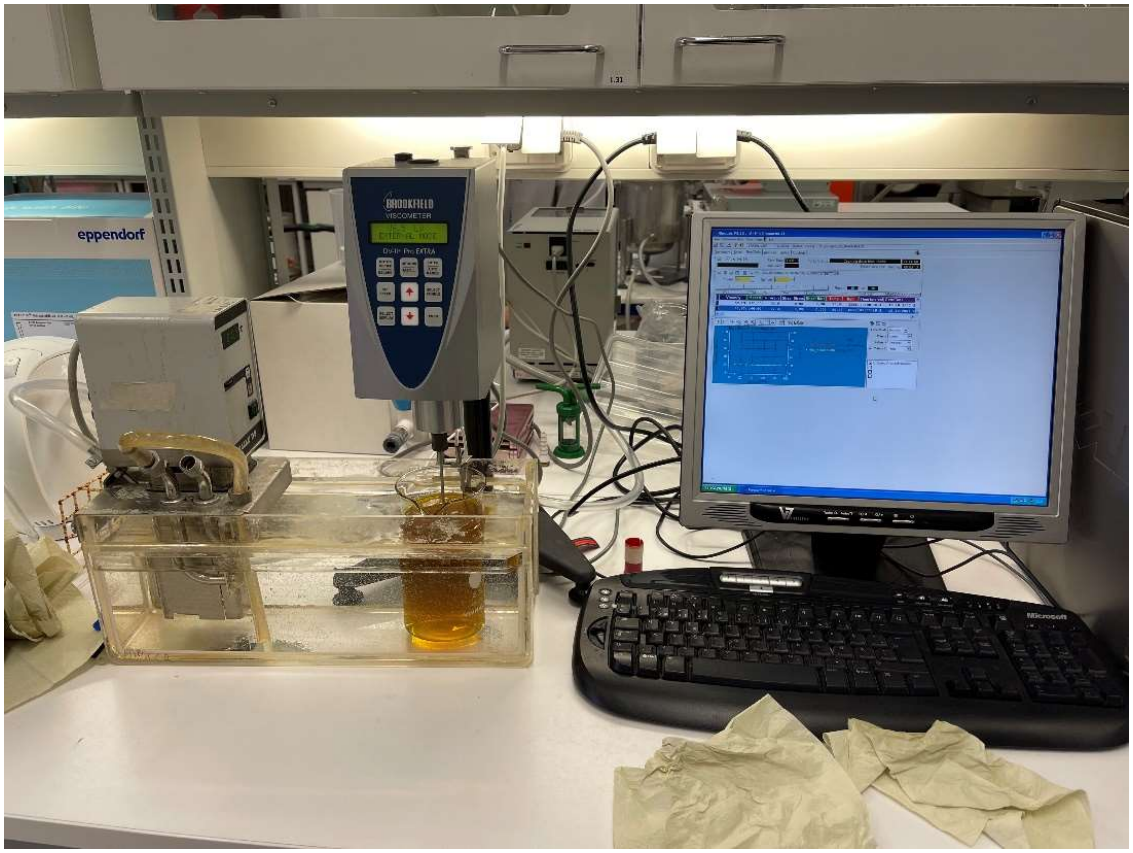

Before the measurement, the oil temperature was raised to 20°C to match the temperature of the oil used in the water model by immersing 500 ml of rapeseed oil in a glass container into a heating circulator. Viscosity was measured by creating a 39-step program where the viscometer speed would increase and decrease from 10 rpm via 200 rpm to 10 rpm. The rotational speed was changed every 10 s by 10 rpm. Figure 11 shows the results of the measured viscosity. The viscosity of the rapeseed oil used was measured at an average of 0.066 Pa·s.

Figure 11 Results of the viscosity measurement

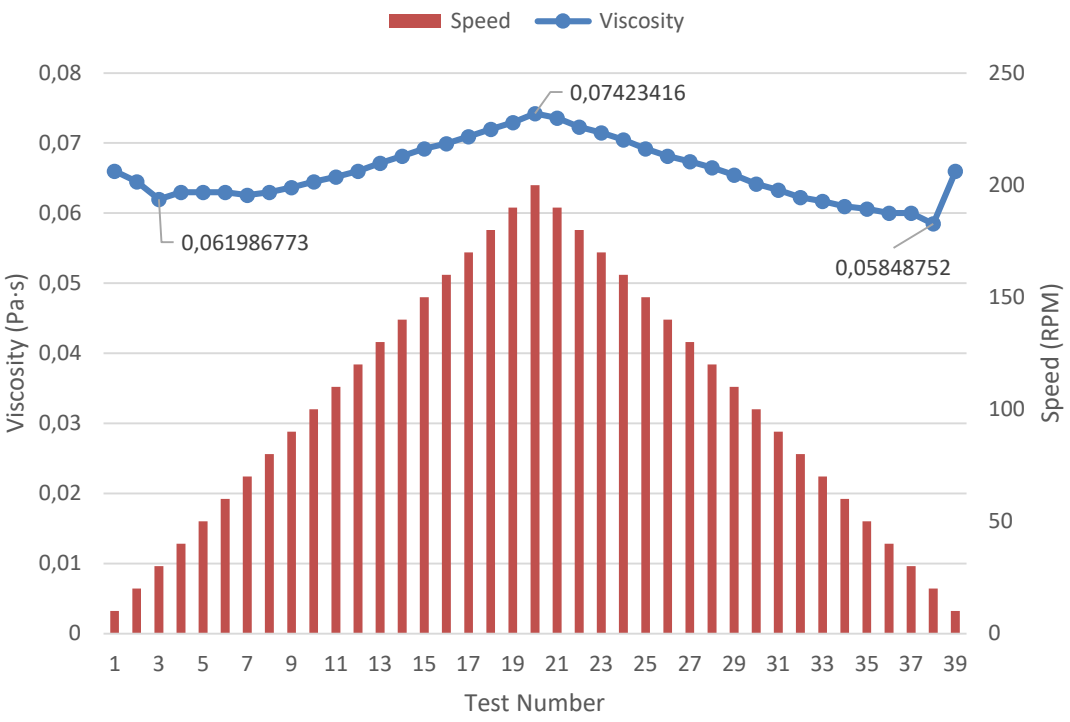

3.4 **Vibration measurements**

To replicate and verify the previous study (Alia, et al. 2019), the same measuring equipment and measurement methods were used. In addition, video recordings were captured during the measurements. Figure 12 shows the facilities and equipment used in the measurement campaign.

Figure 12 . Laboratory where the measurement campaign was carried out

3.4.1 Vibration sensors

Ladle vibrations were measured with eight MMF KS80D mono-axial accelerometers (Figure 13). The accelerometers were calibrated with a PCB 394C06 calibrator, which gave a known amplitude (9.90 m/s^2 ± 1.5 %) and frequency (159.1 Hz ± 0.1 Hz) to make sure that their nominal sensitivity was correct (100 mV/g ± 5 %). The measuring range of the sensors is ±55 g.

Vibration sensors were attached to the PVC blocks which were glued to the water tank, which are visible in Figure 13. PVC blocks were manufactured specially to fit the ladle wall. Total mass of the accelerometer and block is 99 g. The total mass of eight sensors compared to the water tank is so small that it is assumed that it has no impact on the mechanical or vibrational behaviour. Sensors were placed horizontally towards the ladle wall to achieve the highest amplitude (3 % slope).

Figure 13 Accelerometer used in the study

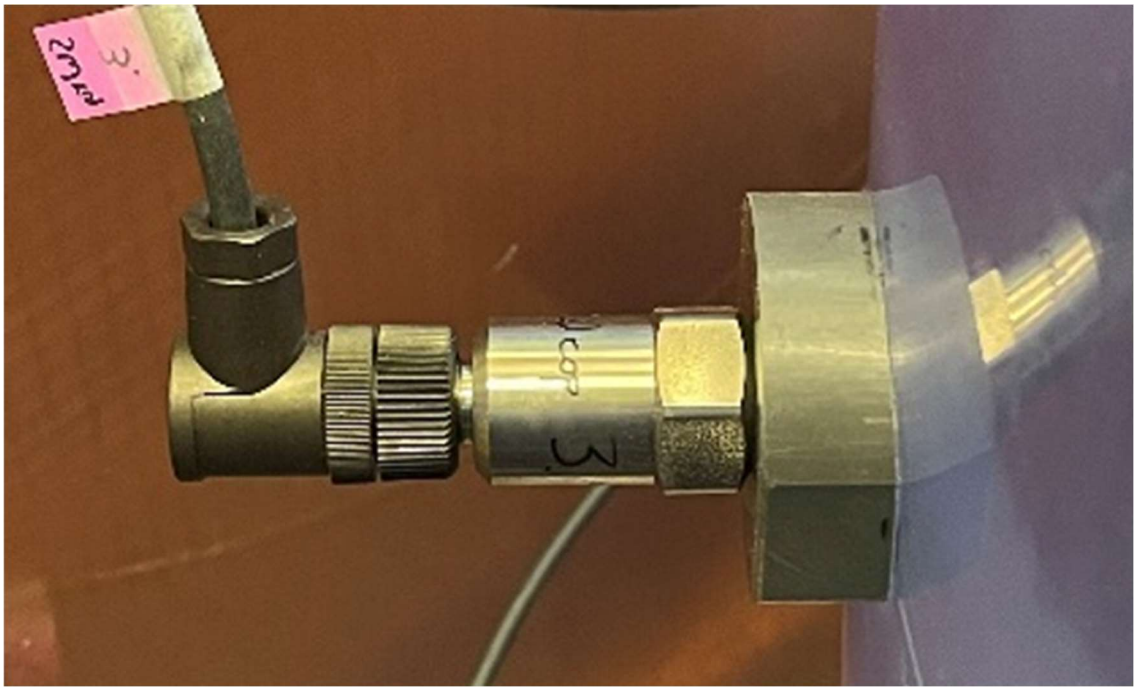

Accelerometers were placed on two levels around the ladle with four sensors per level (Figure 14). Due to the nature of this study as a continuity of the previous research, the positions of the vibration sensors were chosen according to two criteria in the experimental campaign, "the vertical level to the liquid-free surface, and the radial distance to the nozzles and, consequently, to the gas plumes." (Alia, et al. 2019). The lower level of the sensors (*h*1) will always be below the liquid surface, but in this study, the upper level (*h*2) is either at or below. This means that measurements of the ''free space'' won't be made. The *h*1 position is close to the bottom of the ladle and to the gas nozzles (Figure 14).

Figure 14 a) Positions and designation of the accelerometers (h1 = 25 cm and h2 = 54 cm) (Alia, et al. 2019) b) real water model. Two sensors visible from both heights.

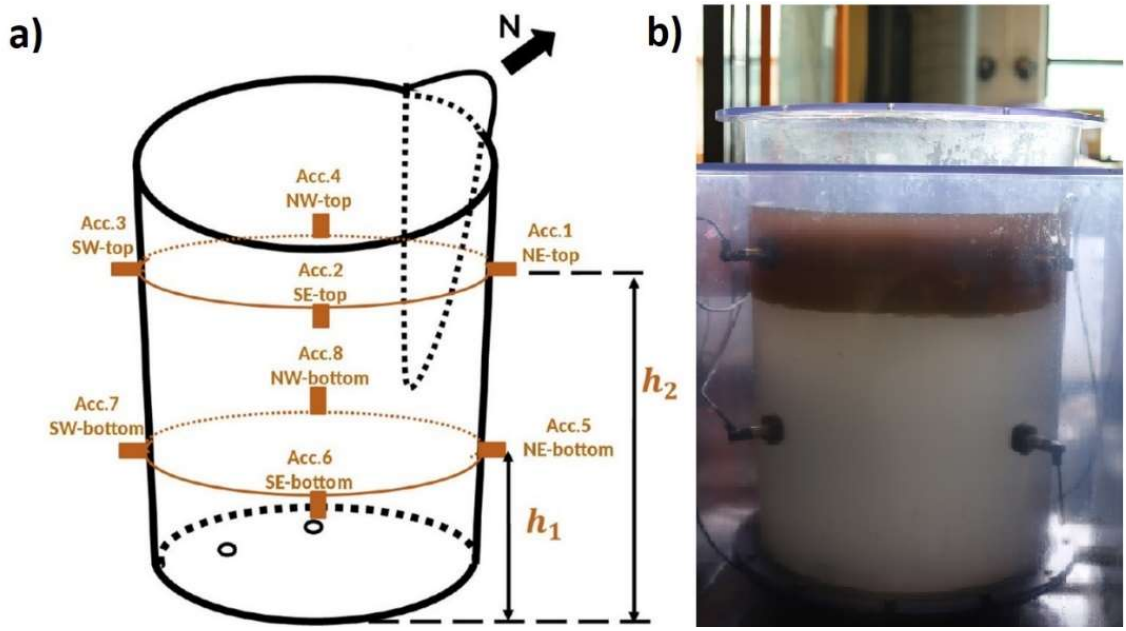

3.4.2 Signal treatment

There were total of 98 tested cases with gas valves open and seven cases that measured oscillation frequency of the ladle. Each of those 98 cases was recorded for 5 min by eight sensors with a sampling frequency of 25.6 kHz. The vibration data was captured using a data acquisition module. The same recording process was performed for each test point (Figure 15).

Figure 15 Timeline of the measurement

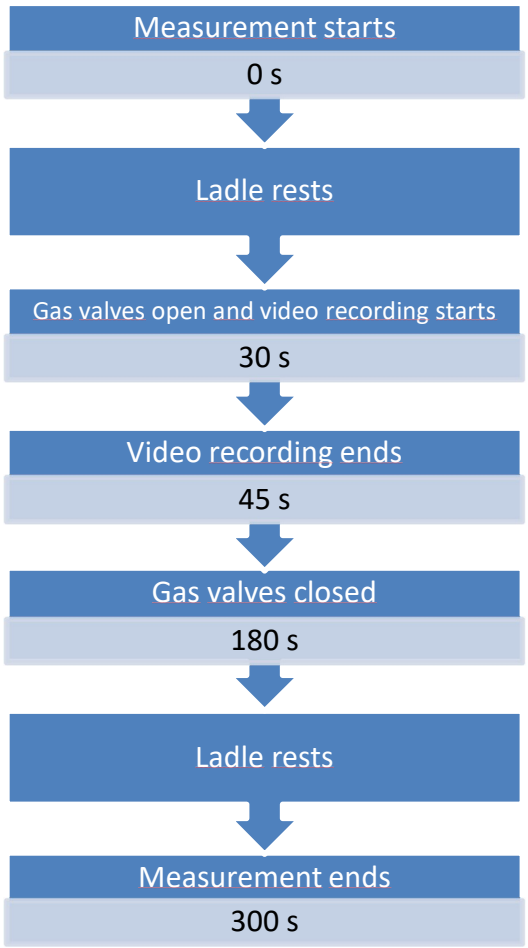

First, the ladle rests for 30 s. At the 30th second, the gas valve was opened, and the recording of the formation of the open eye started. During the 45th second, the video recording stops. The formation of the open eye takes approximately 15 s depending on the thickness of the oil layer. The gas valve is closed at the 210th second. The ladle rests until the end of the measurement at the 300th second.

The vibration data files from the measurement campaign were processed using Python (Appendix 2). To build the dataset, each file had to be cleaned of extra data and the time-specific files had to be merged. The files were merged and rewritten in matrix format. The matrix contains nine columns, the first of which represents the time in seconds when the accelerometers measure the vibration of the water tank. The other eight columns describe the output measured by the sensors in units of m/s^2. The software used in the measurement campaign wrote 60 s of vibration data to each file,

resulting in five files for one run. Since one dataset contained five different files, the first column of the matrix had to be rewritten so that the first row of the matrix starts at 0 s and ends at 300 s (Appendix 3).

For data analysis and visualisation, the amplitude and intensity of the oscillation had to be given an appropriate quantity, root-mean-square (RMS). The RMS values were calculated from the processed files using a Python script (Appendix 4). The values were retrieved from the files in the time interval 40^{th} – 200^{th} second while the mixing takes place in 30^{th} – 210^{th}. The time interval was chosen to keep the gas stirring as constant as possible and to eliminate the transitional phases when the water tank is at rest. In addition, the time interval allows for comparability of the data, as this time interval was used in the original analysis.

4 RESULTS AND DISCUSSION

4.1 Relationship between vibration and process parameters

The graphs used in the results are constructed according to Table 3 and Table 4. Table 3 shows all values calculated from the tests considering the specific oscillation frequency. The calculated values in Table 4 are randomly selected so that there are three different flow rates for each fluid surface, forming a table of twelve runs.

Table 3. RMS values of the specific oscillation frequency

Oil (cm)	A1	A2	A3	A4	A5	A6	A7	A8
0	11.35	7.93	7.45	11.06	4.79	4.31	3.95	4.68
3	8.25	5.40	5.32	8.58	4.70	3.89	3.54	4.42
6	5.96	3.94	4.00	6.26	4.42	3.20	3.03	4.04
9	5.30	3.85	3.92	4.98	4.73	3.42	3.50	4.20

Table 4. RMS values in different cases

Water (cm)	Oil (cm)	Nl/Min	A1	A2	A3	A4	A5	A6	A7	A8
54.00	0.00	5.00	0.14	0.13	0.16	0.18	0.11	0.14	0.11	0.20
54.00	0.00	17.50	0.36	0.33	0.38	0.53	0.29	0.33	0.30	0.53
54.00	0.00	30.00	0.50	0.46	0.54	0.70	0.42	0.45	0.42	0.73
54.00	3.00	5.00	0.18	0.16	0.20	0.25	0.16	0.19	0.16	0.26
54.00	3.00	17.50	0.38	0.36	0.38	0.56	0.38	0.38	0.34	0.52
54.00	3.00	30.00	0.50	0.47	0.52	0.71	0.49	0.49	0.47	0.66
54.00	6.00	5.00	0.16	0.15	0.16	0.23	0.16	0.17	0.16	0.26
54.00	6.00	17.50	0.41	0.36	0.36	0.62	0.37	0.39	0.36	0.55
54.00	6.00	30.00	0.53	0.51	0.50	0.82	0.51	0.54	0.53	0.74
54.00	9.00	5.00	0.14	0.14	0.14	0.22	0.16	0.15	0.15	0.23
54.00	9.00	17.50	0.36	0.31	0.32	0.58	0.33	0.33	0.33	0.49
54.00	9.00	30.00	0.47	0.44	0.46	0.79	0.48	0.46	0.49	0.71

4.1.1 Specific oscillation frequency

The specific oscillation frequency of the water tank was measured to see if the thickness of the oil layer could be determined by hitting the side of the tank (Figure 16) with a mass hammer.

Figure 16 Area where hammer hits took place is marked with a red circle. a) water tank orientation b) real-life model from the campaign

a) **b)**

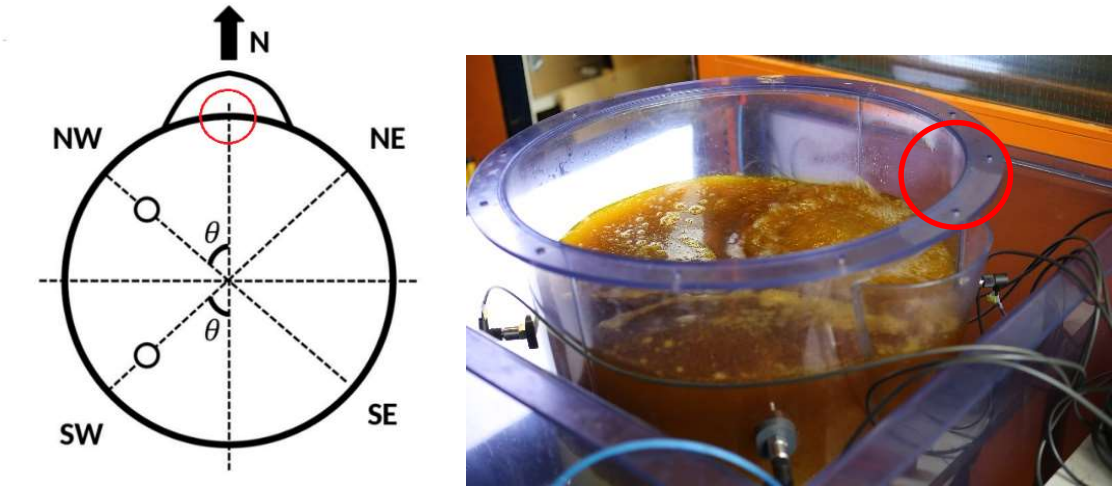

Figure 17 shows that the sensors in the upper layer (Acc. 1 - Acc. 4) are more sensitive to vibration, especially Acc. 1 and Acc. 4. These sensors are next to the impact area, which explains significantly higher RMS values.

When measuring the vibration, if the oil layer is 0, the sensors in the upper layer are not entirely below the liquid surface, but the liquid surface is at the level of the sensor hub. This affects the water tank's vibration behaviour when capturing vibration signals with the top sensors versus the bottom sensors. The top sensors are partly facing the free surface and are not entirely facing the liquid, but the bottom ones are. This means that the bottom sensors are more dampened than the top ones, which leads to higher results of vibration. In Figure 17, it can be clearly seen that the more submerged the sensors are below the liquid surface, the smaller the dispersion of the RMS values is between the sensors

Figure 17 Specific oscillation frequency with all eight sensors and four oil layers

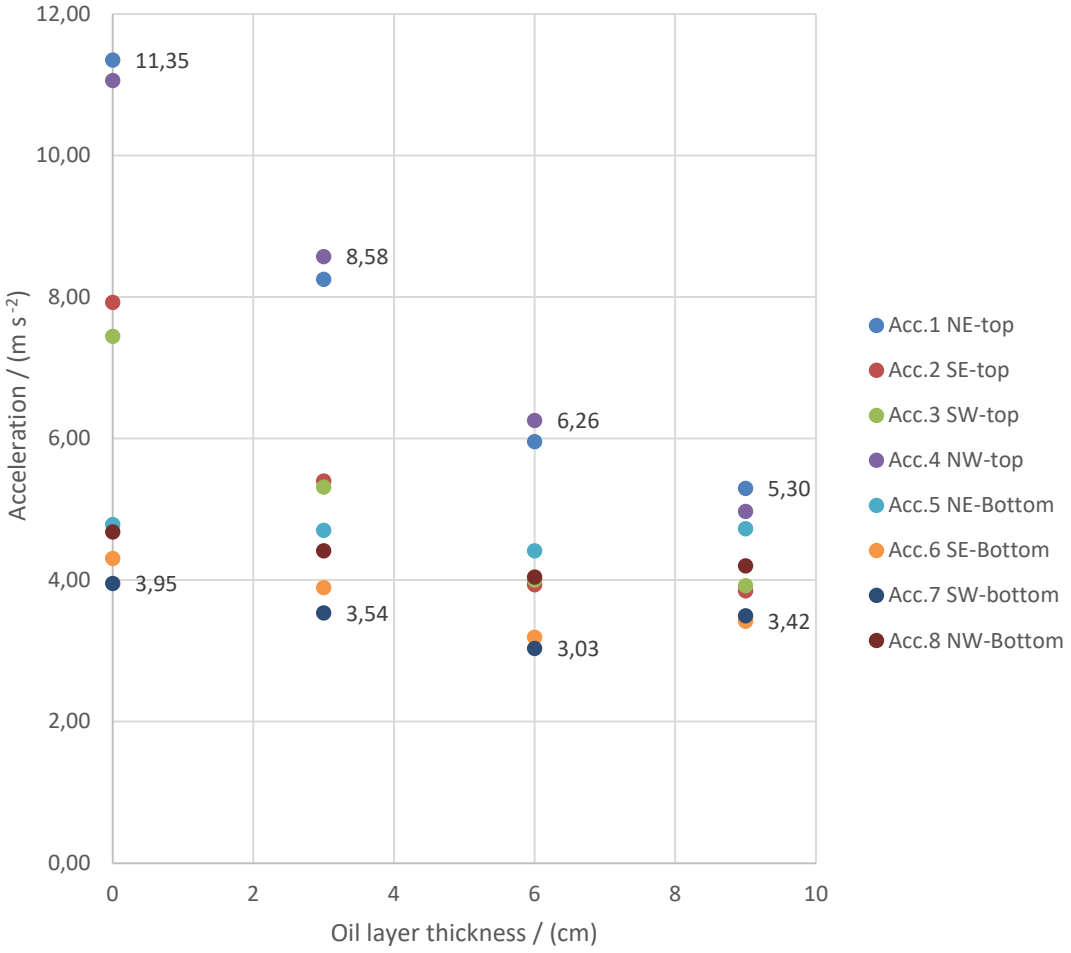

For example, in Figure 17, if the oil-layer thickness is 0 cm, there is only water in the water tank. In this case, the accelerometers of the upper layer are at the level of the liquid surface. In this case, the difference between the RMS values of all eight accelerometers is 7.4 m/s^2. While for an oil layer thickness of 9 cm, with all sensors below the liquid surface, the difference is 1.88 m/s^2. There is a notable difference between surface heights when examining the RMS values from the top layer of accelerometers.

4.1.2 Effect of gas flow rate on vessel vibration

Figure 18 shows how the RMS values of the vibration change in relation to the change in gas flow rate. From Figure 18, it can be seen that the RMS values of the ladle vibration increase in proportion to the increase in gas flow intensity. The obtained data and graphs show that the gas flow intensity versus oscillation is not linear but logarithmic. This has also been proven in previous studies (Alia, et al. 2019).

Figure 18 RMS values of ladle vibration versus gas flow rate with all four liquid surface heights.

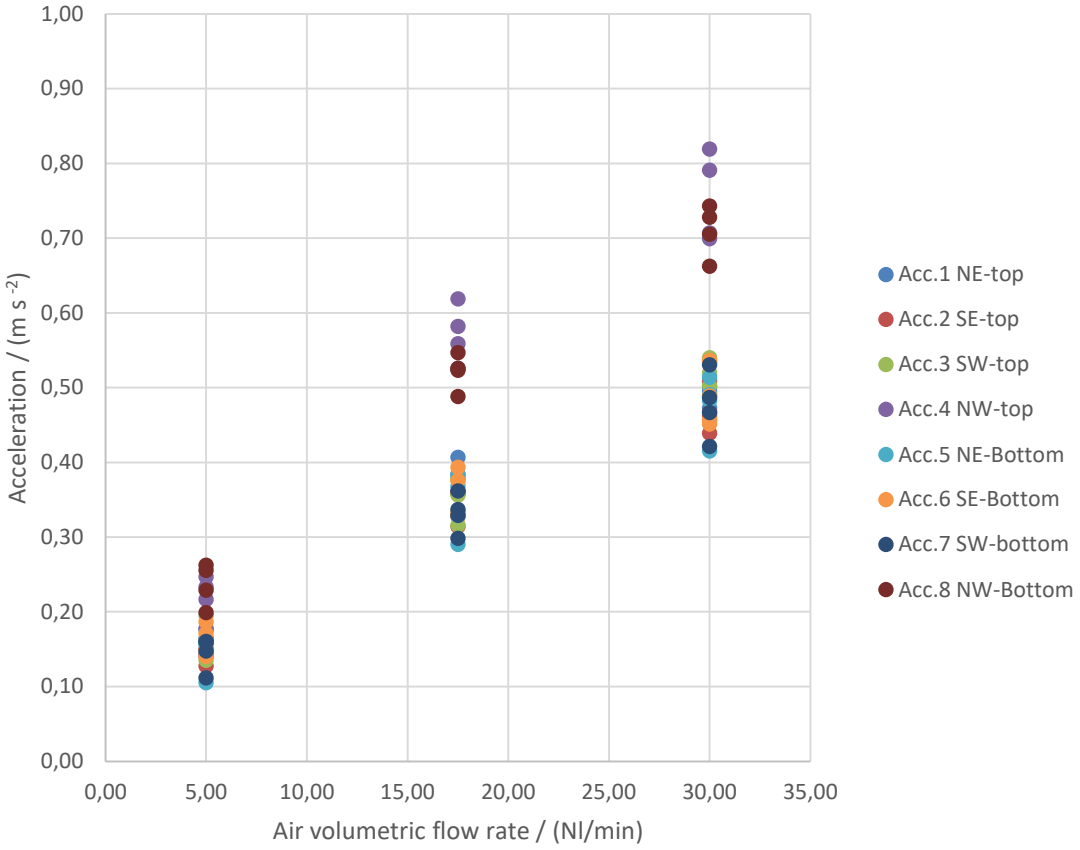

Looking at the increase in RMS values in Figure 18, it can be seen that accelerometers Acc. 4 and Acc. 8 have significantly higher RMS values than the others, especially at higher flow rates of 17.5 Nl/min and 30 Nl/min. This is due to the use of nozzle NW as shown in Figure 7 for the measurements, meaning that the sensors Acc. 4 and Acc. 8 next to the gas plumes.

As in the case of the specific vibration frequency, the upper layer sensors (Acc. 1 - Acc. 4) get higher results than the lower layer sensors (Acc. 5 - Acc. 8). Compared to the other sensors, it can be seen that the position of the sensors is of great importance in relation to the position of the nozzle.

4.1.3 Effect of oil layer thickness on vessel vibration

When you look at vibration from the point of view of the height of the liquid surface, figure 20 shows the RMS values of the vibration with respect to the oil layer heights. Figure 20a shows that the amount of vibration increases slightly at a flow rate of 5 Nl/min when oil is added to the liquid surface (heights 0 cm and 3 cm). As more oil is added to the tank (heights 6 cm and 9 cm) the vibration intensity starts to decrease slowly. Observing the change in vibration from the perspective of the oil layer at higher flow rates in Figures 20b and 20c. A similar change in vibration intensity can be observed, but in these cases, the increase continues up to a height of 6 cm until it starts to decrease at a height of 9 cm. A similar phenomenon has occurred in previous cases (Alia, Pylvänäinen, Visuri, John, & Ollila, 2019). This is interesting because, in Figure 17, it can be seen that the higher the liquid surface is, the lower values were measured.

Figure 19 RMS values of the vibration versus four surface levels. Volumetric flowrate of air a) 5 Nl / min b) 17.5 Nl / min c) 30 Nl / min

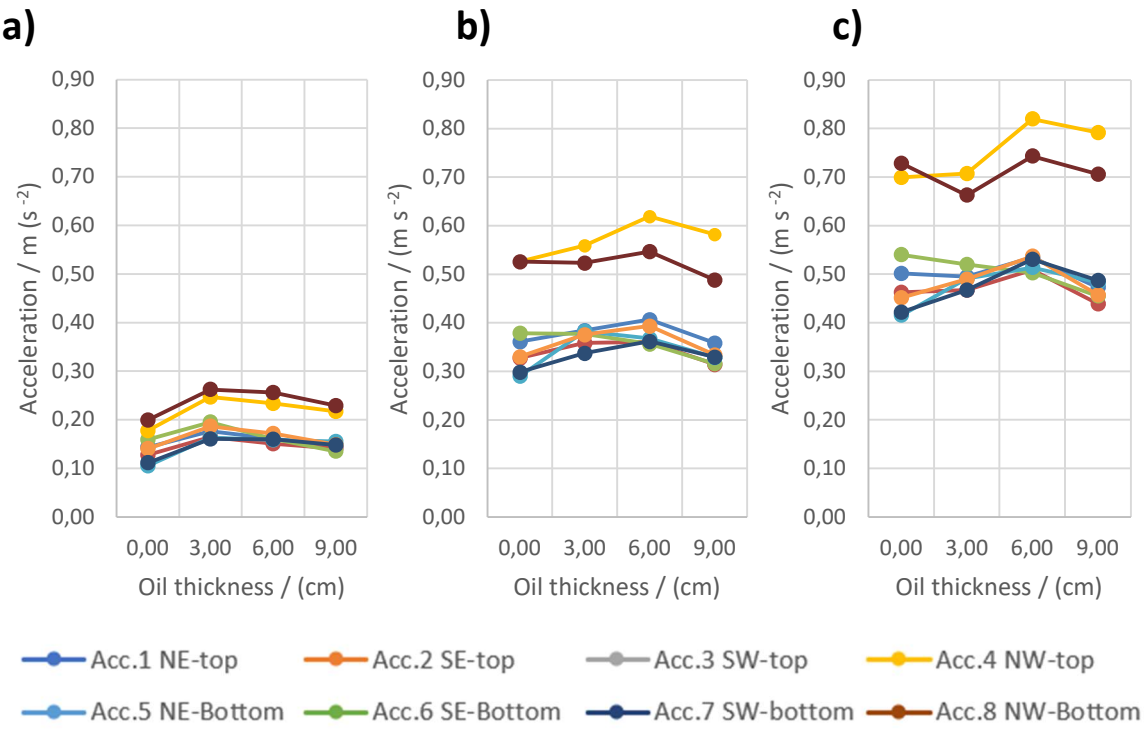

5 CONCLUSIONS

The aim of the study was to study the effect of slag on the vibration of a steel ladle. To this end, experiments with a 1:5 scale water model of a 150-ton steel ladle were conducted with a tank under room temperature conditions using different air flow rates and oil layer thicknesses. During the experiments, the water model was monitored using eight accelerometers, i.e., two levels of accelerometers with four accelerometers per level.

The measurement results, expressed as RMS values, show, as in previous studies, that the thickness of the oil layer and, in general, the height of the liquid surface play a role in the vibration of the tank. The most evident results were seen when looking at the specific oscillation frequency. The thicker the oil layer on the surface of the water tank, the lower the RMS values obtained. Although the most significant changes were observed in the sensors located near the impact area, other sensors can also be used to detect the change in the oil layer. In general, the dispersion of the measurement results decreases and the results level off significantly with increasing surface depth. It remains an open question whether the measurement results are further smoothed as the liquid level rises and how much of an effect the water level has. As already noted in previous studies, it is difficult to observe any clear recurring trend in the contribution of vibration intensity to the height of the oil surface (Alia, et al. 2019). However, it can be said that changes are noticeable. When looking at the RMS values from the point of view of the oil layer thickness, it can be seen that the sensors in the lowest layer initially get higher

results with oil than without oil. After the vibration intensity has increased during the first oil addition, it can be observed that when oil is added again, the vibration intensity starts to decrease.

Thus, based on previous studies and the results presented, it can be concluded that the thickness of the oil layer affects vibration intensity in a way that could be identified by accelerometers. It is essential to mention that the measurement results are indeed dependent on the position of the accelerometers. As shown in the results, accelerometers close to the nozzle and the gas flow are more sensitive to changes in process parameters than those on the opposite side.

The compiled dataset provides a basis for studies on the gas-stirring related to the ladle vibration. The documentation of this work can be used for further analysis of the dataset resulting from the measurement campaign. In addition, the dataset can be used to analyse video recordings captured from the open-eye formation.

REFERENCES.

Alia, N., Pylvänäinen, M., Visuri, V.-V., John, V., & Ollila, S. (2019). Vibrations of a laboratory-scale gas-stirred ladle with two eccentric nozzles and multiple sensors. *Journal of Iron and Steel Research International, 26*, 1031-1040. Retrieved from http://urn.fi/urn:nbn:fi-fe202003067582

Anagbo, P. E.;Brimacombe, J. K.;& Castillejos, A. H. (1989). A Unified Representation of Gas Dispersion in Upwardly Injected Submerged Gas Jets. *Canadian Metallurgical Quarterly, 28*, 323-330. https://doi.org/10.1179/cmq.1989.28.4.323

Britannica. (2021, April 9). *Secondary steelmaking*. Retrieved from https://www.britannica.com/technology/steel/Secondary-steelmaking

Heikkinen, E.-P. (2021). Korkealämpötilaprosessit: Pyrometallurgiset jalostusprosessit. Oulu, Pohjois-Pohjanmaa, Suomi.

Jones, B., & Nachtsheim, C. J. (2017, April). Effective Design-Based Model Selection for Definitive Screening Designs. *Technometrics, 59*, 319-329. https://doi.org/10.1080/00401706.2016.1234979

Järvinen, M., Kärnä, A., Visuri, V.-V., Sulasalmi, P., Heikkinen, E.-P., Pääskylä, K., . . . Fabritius, T. (2014). A Novel Approach for Numerical Modeling of the CAS-OB Process: Process Model for the Heat-Up Stage. *ISIJ International, 54*, 2263-2272. Retrieved from https://doi.org/10.2355/isijinternational.54.2263

Metallinjalostajat ry. (2014). *Teräskirja.* Helsinki: Metallinjalostajat ry.

O'Malley, R. J. (2017). Inclusion Evolution and Removal in Ladle Refining. *Inclusion Engineering, AIS Tech2017* (p. 2). Nashville, TN: Missouri University of Science & Technology. Retrieved from https://www.researchgate.net/publication/318311375_Inclusion_Evolution_and_Removal_in_Ladle_Refining

Palovaara, T. (2017). *Physical modelling of gas injection in a ladle (Master's thesis).* Oulu: University of Oulu. Noudettu osoitteesta http://urn.fi/URN:NBN:fi:oulu-201706012288

Palovaara, T.;Visuri, V.-V.;& Fabritius, T. (June 2018). Physical modelling of gas injection in a ladle. *Proceedings of the 7th International Congress on Science and Technology of Steelmaking, .* Venice, Italy: Associazione Italiana di Metallurgia.

Ramasetti, E. K. (2019). *Modelling of open-eye formation and mixing phenomena in a gas-stirred ladle for different operating parameters (Doctoral dissertation).* Oulu: University of Oulu. Noudettu osoitteesta http://urn.fi/urn:isbn:9789526223568

Ramasetti, E. K., Visuri, V.-V., Sulasalmi, P., Mattila, R., & Fabritius, T. (2018, November). Modeling of the Effect of the Gas Flow Rate on the Fluid Flow and Open-Eye Formation in a Water Model of a Steelmaking Ladle. *steel research international, 90*, 1800365. doi:10.1002/srin.201800365

Stolte, G. (2002). *Secondary metallurgy: Fundamentals.* Düsseldorf: Stahleisen GmbH.

Szekely, J., Carlsson, G., & Helle, L. (1989). *Ladle Metallurgy.* New York: Springer.

APPENDICES

Appendix 1: Design of experiment

Test nuber	Oil-layer thickness (cm)	Air volumetric flow rate (Nl/min)	File name (csv.)	File name (video)	NOTICE: Water surface height 54cm. Air flow NW-nozzle.
HIT 1	0	NO	isku1_22_t		No video recording!
1	0	30	ajo1_22_t	Ajo 1	
2	0	17.5	ajo2_22_t	Ajo 2	
3	0	17.5	ajo3_22_t	Ajo 3	
4	0	17.5	ajo4_22_t	Ajo 4	
5	0	30	ajo5_22_t	Ajo 5	
6	0	5	ajo6_22_t	Ajo 6	
7	0	5	ajo7_22_t	Ajo 7	
8	0	17.5	ajo8_22_t	Ajo 8	
9	0	5	ajo9_22_t	Ajo 9	
10	0	5	ajo10_22_t	Ajo 10	
11	0	30	ajo11_22_t	Ajo 11	
12	0	30	ajo12_22_t	Ajo 12	
13	0	5	ajo13_22_t	Ajo 13	
14	0	30	ajo14_22_t	Ajo 14	
15	0	17.5	ajo15_22_t	Ajo 15	
HIT 2	57	NO	isku2_22_t		Oil level 0cm (no video recording)
15.1	57	30	vesiajo1_22_t		Oil level 0cm (no video recording)
15.2	57	5	vesiajo2_22_t		Oil level 0cm (no video recording)
15.3	57	17.5	vesiajo3_22_t		Oil level 0cm (no video recording)
HIT 3	60	NO	isku3_22_t		Oil level 0cm (no video recording)
15.4	60	5	vesiajo4_22_t		Oil level 0cm (no video recording)
15.5	60	30	vesiajo5_22_t		Oil level 0cm (no video recording)
15.6	60	17.5	vesiajo6_22_t		Oil level 0cm (no video recording)
HIT 4	63	NO	isku4_22_t		Oil level 0cm (no video recording)
15.7	63	30	vesiajo7_22_t		Oil level 0cm (no video recording)
15.8	63	17.5	vesiajo8_22_t		Oil level 0cm (no video recording)
15.9	63	5	vesiajo9_22_t		Oil level 0cm (no video recording)
16	0,3	19,4	ajo16_22_t	Ajo 16	Model testpoint
17	1	5.6	ajo17_22_t	Ajo 17	Model testpoint
18	1,9	25.5	ajo18_22_t	Ajo 18	Model testpoint
HIT 5	3	NO	isku5_22_t		No video recording!
19	3	17.5	ajo19_22_t	Ajo 19	
20	3	30	ajo20_22_t	Ajo 20	

21	3	17.5	ajo21_22_t	Ajo 21	
22	3	17.5	ajo22_22_t	Ajo 22	
23	3	5	ajo23_22_t	Ajo 23	
24	3	5	ajo24_22_t	Ajo 24	
25	3	30	ajo25_22_t	Ajo 25	
26	3	5	ajo26_22_t	Ajo 26	
27	3	30	ajo27_22_t	Ajo 27	
28	3	30	ajo28_22_t	Ajo 28	
29	3	17.5	ajo29_22_t	Ajo 29	
30	3	30	ajo30_22_t	Ajo 30	
31	3	5	ajo31_22_t	Ajo 31	
32	3	30	ajo32_22_t	Ajo 32	
33	3	30	ajo33_22_t	Ajo 33	
34	3	5	ajo34_22_t	Ajo 34	
35	3	30	ajo35_22_t	Ajo 35	
36	3	5	ajo36_22_t	Ajo 36	
37	3	17.5	ajo37_22_t	Ajo 37	
38	3	5	ajo38_22_t	Ajo 38	
39	3	30	ajo39_22_t	Ajo 39	
40	3	30	ajo40_22_t	Ajo 40	
41	3	5	ajo41_22_t	Ajo 41	
42	3	5	ajo42_22_t	Ajo 42	
43	3	5	ajo43_22_t	Ajo 43	
44	4,1	20.4	ajo44_22_t	Ajo 44	Model testpoint
45	5,3	22.5	ajo45_22_t	Ajo 45	Model testpoint
46	5,5	28.8	ajo46_22_t	Ajo 46	Model testpoint
HIT 6	6	NO	isku6_22_t		No video recording!
47	6	17.5	ajo47_22_t	Ajo 47	
48	6	5	ajo48_22_t	Ajo 48	
49	6	30	ajo49_22_t	Ajo 49	
50	6	17.5	ajo50_22_t	Ajo 50	
51	6	17.5	ajo51_22_t	Ajo 51	
52	6	5	ajo52_22_t	Ajo 52	
53	6	30	ajo53_22_t	Ajo 53	
54	6	5	ajo54_22_t	Ajo 54	
55	6	30	ajo55_22_t	Ajo 55	
56	6	30	ajo56_22_t	Ajo 56	
57	6	5	ajo57_22_t	Ajo 57	
58	6	5	ajo58_22_t	Ajo 58	
59	6	17.5	ajo59_22_t	Ajo 59	
60	6	17.5	ajo60_22_t	Ajo 60	
61	6	30	ajo61_22_t	Ajo 61	
62	7	25.5	ajo62_22_t	Ajo 62	Model testpoint
63	7,3	17.8	ajo63_22_t	Ajo 63	Model testpoint
64	7,9	18.1	ajo64_22_t	Ajo 64	Model testpoint
HIT 7	9	NO	isku7_22_t		No video recording!

65	9	5	ajo65_22_t	Ajo 65
66	9	17.5	ajo66_22_t	Ajo 66
67	9	30	ajo67_22_t	Ajo 67
68	9	5	ajo68_22_t	Ajo 68
69	9	30	ajo69_22_t	Ajo 69
70	9	30	ajo70_22_t	Ajo 70
71	9	30	ajo71_22_t	Ajo 71
72	9	5	ajo72_22_t	Ajo 72
73	9	5	ajo73_22_t	Ajo 73
74	9	5	ajo74_22_t	Ajo 74
75	9	17.5	ajo75_22_t	Ajo 75
76	9	5	ajo76_22_t	Ajo 76
77	9	30	ajo77_22_t	Ajo 77
78	9	30	ajo78_22_t	Ajo 78
79	9	30	ajo79_22_t	Ajo 79
80	9	30	ajo80_22_t	Ajo 80
81	9	30	ajo81_22_t	Ajo 81
82	9	30	ajo82_22_t	Ajo 82
83	9	17.5	ajo83_22_t	Ajo 83
84	9	17.5	ajo84_22_t	Ajo 84
85	9	5	ajo85_22_t	Ajo 85
86	9	17.5	ajo86_22_t	Ajo 86
87	9	5	ajo87_22_t	Ajo 87
88	9	5	ajo88_22_t	Ajo 88
89	9	5	ajo89_22_t	Ajo 89

Appendix 2: Python script for merging the vibration data

```
from os import listdir
from os.path import isfile, join
import os


import csv

def main():

    data = []

    iskut = ["isku1_22-02-14_1146_1"]

    mypath = "E:\Vdata"
    onlyfiles = [f for f in listdir(mypath) if isfile(join(mypath, f))]


    ajo_list = [1, 16, 19, 47, 65, 90]

    vesi_list = [1,4,7,10]

    ajo_nro = 0
    vesi_nro = 0
    count = 0

    for isku_idx in range(1,8,1):

        count = 0

        isku_s = "isku" + str(isku_idx) + "_22"
        print(isku_s)

        for isku_file in onlyfiles:
            if isku_file.startswith(isku_s) == True:

                with open(isku_file, newline = '') as isku:
                        isku_reader = csv.reader(isku, delimiter="\t")

                        for line_i in isku_reader:

                            if count > 22:
                                data.append(line_i)
                            count += 1


        with open(isku_s, 'w', newline='') as csvfile:
            writer = csv.writer(csvfile)
            writer.writerows(data)
```

```
data.clear()


if isku_idx < 2 or isku_idx > 4:
    for ajo_idx in range(ajo_list[ajo_nro],ajo_list[ajo_nro+1],1):

        file_s = "ajo" + str(ajo_idx) + "_22"
        print(file_s)

        for ajo_file in onlyfiles:

            count = 0
            if ajo_file.startswith(file_s) == True:
                #print(d)
                with open(ajo_file, newline = '') as ajo:
                    ajo_reader = csv.reader(ajo, delimiter="\t")

                    for line_a in ajo_reader:
                        if count > 22:
                            data.append(line_a)
                        count += 1

        with open(file_s, 'w', newline='') as csvfile:
            writer = csv.writer(csvfile)
            writer.writerows(data)

        data.clear()
    ajo_nro += 1


if isku_idx > 1 and isku_idx < 5:
    for ajo_idx in range(vesi_list[vesi_nro],vesi_list[vesi_nro+1],1):

        vesi_s = "vesiajo" + str(ajo_idx) + "_22"
        print(vesi_s)

        for vesi_file in onlyfiles:

            count = 0
            if vesi_file.startswith(vesi_s) == True:
                #print(d)
                with open(vesi_file, newline = '') as vesi:
                    vesi_reader = csv.reader(vesi, delimiter="\t")

                    for line_v in vesi_reader:
                        if count > 22:
                            data.append(line_v)
                        count += 1
```

```
                with open(vesi_s, 'w', newline='') as csvfile:
                    writer = csv.writer(csvfile)
                    writer.writerows(data)

                data.clear()
            vesi_nro += 1

        if isku_idx == 4:
             for ajo_idx in range(ajo_list[ajo_nro],ajo_list[ajo_nro+1],1):

                file_s = "ajo" + str(ajo_idx) + "_22"
                print(file_s)

                for ajo_file in onlyfiles:

                    count = 0
                    if ajo_file.startswith(file_s) == True:
                        #print(d)
                        with open(ajo_file, newline = '') as ajo:
                            ajo_reader = csv.reader(ajo, delimiter="\t")

                            for line_a in ajo_reader:
                                if count > 22:
                                    data.append(line_a)
                                count += 1

                with open(file_s, 'w', newline='') as csvfile:
                    writer = csv.writer(csvfile)
                    writer.writerows(data)

                data.clear()
             ajo_nro += 1

main()
```

Appendix 3: Python script for rewriting columns

```
#%%
import pandas as pd
import numpy as np
import matplotlib.pyplot as plt
import csv

#%%
header_list = [0,1,2,3,4,5,6,7,8]
file_list = []

for i in file_list:
    f_name = i
    df = pd.read_csv(f_name, names=header_list)
    df = df.to_numpy()
    l_ajo = df.shape[0]

    fs = 25600

    t = np.linspace(0, l_ajo*(1/fs), l_ajo)

    df[:,0] = t

    with open(f_name + "_t.csv", 'w', newline='') as csvfile:
                writer = csv.writer(csvfile)
                writer.writerows(df.tolist())
```

Appendix 4: Python script for calculating RMS values

```
#%%
import pandas as pd
import numpy as np
import csv

#%%
header_list = [0,1,2,3,4,5,6,7,8]
file_list = []

def rms_detrend(x):
    return np.sqrt(sum(y**2 for y in x)/len(x))

ALKU = 1024001
LOPPU = 5120001

for i in file_list:
    f_name = i

    accdf =pd.read_csv(f_name, names=header_list)

    accdf = accdf.drop([0],axis=1)
    accdf = accdf.iloc[ALKU:LOPPU]

    accdf['ACC_RMS'] = accdf.apply(rms_detrend,axis=1)

    testi =  accdf.apply(rms_detrend)

    accdf = accdf.drop([1,2,3,4,5,6,7,8], axis=1)

    with open(f_name + "_rmsrow.csv", 'w', newline='') as csvfile:
       writer = csv.writer(csvfile)
       writer.writerows(accdf.values.tolist())

    with open(f_name + "_rmscol.csv", 'w', newline='') as csvfile:
       writer = csv.writer(csvfile)
       writer.writerow(testi.tolist())
```